







Article

# Bending of Light by Magnetars within Generalized Born–Infeld Electrodynamics: Insights from the Gauss–Bonnet Theorem

Nurzada Beissen <sup>1</sup>, Tursynbek Yernazarov <sup>1,†</sup>, Manas Khassanov <sup>1,\*,†</sup>, Saken Toktarbay <sup>1,2,†</sup>,  
Aliya Taukenova <sup>1</sup> and Amankhan Talkhat <sup>1,†</sup>

<sup>1</sup> Institute for Experimental and Theoretical Physics, Al-Farabi Kazakh National University, Almaty 050040, Kazakhstan; nurzada.beissen@kaznu.edu.kz (N.B.); tursynbek.yernazarov.t@kaznu.kz (T.Y.); saken.toktarbay@kaznu.edu.kz (S.T.)

<sup>2</sup> Department of Physics, Kazakh National Women’s Teacher Training University, Almaty 050000, Kazakhstan

\* Correspondence: khassanov.manas@kaznu.kz

† These authors contributed equally to this work and are co-first authors.

**Abstract:** We compute the weak bending angle of light within generalised Born–Infeld electrodynamics as it passes through the equatorial plane of a magnetic dipole. We start by considering the refractive index associated with the dipole within generalised Born–Infeld electrodynamics. Then, we calculate the Gaussian optical curvature based on these refractive indices. Using the Gauss–Bonnet theorem, we derive a formula to quantify the deflection angle in the presence of a strong magnetic field from a dipole. Our results align with results obtained through traditional geometric optics techniques, underscoring the importance of the Gauss–Bonnet theorem as a versatile tool for solving intricate problems in modern theoretical research. We apply our theoretical deflection angle formula to estimate the light bending in magnetars listed in the McGill catalogue, providing insights into the behaviour of light in environments with strong magnetic fields.

**Keywords:** Born–Infeld electrodynamics; refractive indices; magnetar; Gauss–Bonnet theorem



**Citation:** Beissen, N.; Yernazarov, T.; Khassanov, M.; Toktarbay, S.; Taukenova, A.; Talkhat, A. Bending of Light by Magnetars within Generalized Born–Infeld Electrodynamics: Insights from the Gauss–Bonnet Theorem. *Symmetry* **2024**, *16*, 132. <https://doi.org/10.3390/sym16010132>

Academic Editor: Eduardo Guendelman

Received: 1 December 2023

Revised: 11 January 2024

Accepted: 18 January 2024

Published: 22 January 2024



**Copyright:** © 2024 by the authors. Licensee MDPI, Basel, Switzerland. This article is an open access article distributed under the terms and conditions of the Creative Commons Attribution (CC BY) license (<https://creativecommons.org/licenses/by/4.0/>).

## 1. Introduction

The nonlinear theory of the electromagnetic field was developed by Born and Infeld to address the issue of the infinite energy associated with a point charge in classical electrodynamics [1–3]. Additionally, nonlinearity in strong fields arises due to vacuum polarisation in quantum electrodynamics, which is described in the classical limit by the Euler–Heisenberg Lagrangian [4,5]. In nonlinear electrodynamics, the speed of light varies depending on the field strength. In the Born–Infeld theory, nonlinearity becomes significant at field strengths on the order of  $10^{20}$  V/m [6], corresponding to magnetic fields of around  $10^{11}$  T. Nonlinear effects in the quantum electrodynamics of a vacuum begin to manifest themselves at critical magnetic field values of  $B_c = \frac{m_e^2 c^2}{e\hbar} \approx 4.4 \times 10^9$  T.

Experimental attempts to verify nonlinear electrodynamics [7–9] are still ongoing. However, convincing confirmations of nonlinear effects have not been achieved in laboratories because of the requirement for extremely high critical-field values. However, magnetars [10–13] provide another opportunity to test the effects of nonlinear electrodynamics with magnetic field strengths on the order of  $B = 10^{11}$  T.

In geometric optics, the change in the path of light is explained by constant changes in the refractive index. This method has been successfully employed in several works, even when dealing with different spacetime properties. When there is a refractive-index gradient, geometric optics methods can be applied to determine the angle of deviation [14–17]. In the case of a strong electromagnetic field, quantum nonlinear electrodynamics leads to polarisation effects and the bending of light in a vacuum. For instance, in [18–21], the angle of light deviation was calculated when passing through the magnetic dipole equator.

However, an alternative method proposed by Gibbons and Werner [22] can be used to calculate the deflection angle of light in nonlinear electrodynamics. This method is based on the use of the Gauss–Bonnet theorem (GBT) to determine the deflection angle. In this approach, the deflection angle is considered a global phenomenon through integration beyond the path of light. Werner applied it to asymptotically flat stationary metrics, such as Kerr black holes [23]. This methodological approach is more complex and uses Finsler–Randers geometry. It also requires the application of the Nazimov technique to create a Riemannian manifold that touches the Randers manifold [23]. It is worth noting that Werner further adapted his method for asymptotically non-flat stationary fields, including the presence of topological anomalies, such as a rotating cosmic string and a rotating global monopole [24–28]. It should be noted that the GBT has also been used to determine the deflection angle of light in the case of a weak field of a charged black hole where nonlinearity was induced by the charge [29,30].

In our study, we employ the Gibson and Werner approach to calculate the deflection angle in the nonlinear electrodynamics of a vacuum using an effective Riemannian manifold. This article is structured as follows: After a brief introduction to the generalised Born–Infeld Lagrangian (classical + quantum) given in Section 2, we investigate the effective refractive index during the propagation of light in a background magnetic field induced by a magnetic dipole. In Section 3, we compute Gaussian optical curvatures based on the effective refractive index and optical metric, followed by the utilisation of the GBT method to obtain the deflection angle. In Section 4, we implement the derived formula for the deflection angle with reference to specific magnetars from the McGill catalogue. In Section 5, we provide a summation of our outcomes.

## 2. The Refractive Index of Born–Infeld Nonlinear Electrodynamics

In recent developments within the field of electrodynamics, several models have been introduced to extend and generalise the Born–Infeld (BI) model [31–35].

Generalised Born–Infeld nonlinear electrodynamics (GBI NED) is a theory explaining how a straight laser beam moves through an external sideways magnetic field [36]. This model includes two key parameters. The GBI model predicts the effect of vacuum birefringence, which is when the light’s polarisation plane turns as it goes through a magnetic field. The highest limits for the model’s parameters were determined using experimental results from the BRST and PVLAS Collaborations [36–38].

We consider the Lagrangian density of GBI as follows [36]:

$$\mathcal{L} = \beta^2 \left( 1 - \sqrt{1 + \frac{2S}{\beta^2} - \frac{P^2}{\beta^2 \gamma^2}} \right), \quad (1)$$

where  $\beta$  and  $\gamma$  are two different nonlinearity parameters and have the dimension of the field strength.  $S$ ,  $P$  are Lorentz invariants [1,39]. Note that Equation (1) represents the nonlinear model of the electrodynamic theory for strong electromagnetic fields.

In addition, following notations in [36], for the small parameters  $\beta^{-2}S$  and  $\beta^{-2}\gamma^{-2}P^{-2}$ , the Lagrangian density of GBI (1) becomes the approximate BI Lagrangian density with quantum corrections that leads to the effective Lagrangian. If  $\beta \neq \gamma$ , this model leads to birefringence. Furthermore, when the parameters  $\beta = \gamma$ , the vacuum birefringence vanishes, aligning with BI electrodynamics. The GBI parameters are given as

$$\frac{1}{\beta^2} = \frac{1}{\beta_0^2} + \frac{16}{45} \frac{\alpha^2}{m_e^4}, \quad \frac{1}{\gamma^2} = \frac{1}{\beta_0^2} + \frac{28}{45} \frac{\alpha^2}{m_e^4}, \quad (2)$$

where  $\beta_0$  is the classical Born–Infeld parameter characterising the possible maximum value of the field strength,  $\alpha$  is the fine structure constant, and  $m_e$  denotes the electron mass.

It is clear that when the parameter  $\beta_0 \rightarrow \infty$ , then the effective BI Lagrangian density reduces to the Euler–Heisenberg Lagrangian, which corresponds to the one-loop corrections in classical electrodynamics (EH NED).

The trajectory of light can be calculated through an effective index of refraction, as proven by Kruglov [36], and for an electromagnetic wave, when its polarisation is perpendicular and parallel to the external magnetic field  $\vec{B}$ , the index can be written as follows:

$$n_{\perp} = \left(1 + \frac{\vec{B}^2}{\beta^2}\right)^{1/2}, \quad n_{\parallel} = \left(1 + \frac{\vec{B}^2}{\gamma^2}\right)^{1/2}. \quad (3)$$

Moreover, in the case of the smallness of the parameters  $\vec{B}^2/\beta^2$  and  $\vec{B}^2/\gamma^2$ , we can write the effective indexes of refraction as

$$n_{\perp} \approx 1 + \frac{\vec{B}^2}{2\beta^2}, \quad n_{\parallel} \approx 1 + \frac{\vec{B}^2}{2\gamma^2}. \quad (4)$$

This calculation includes nonlinear effects in the order of  $\beta^{-2}$  and  $\gamma^{-2}$  approximations. The expression shows that the refractive index directly depends on the characteristics of the magnetic field. Therefore, in our subsequent calculations, we will focus on the background magnetic field caused by a magnetic dipole. Furthermore, expanding the expression into a series using the small parameters  $\beta^{-2}$  and  $\gamma^{-2}$  is sufficient for calculating the light-bending angle caused by a magnetar. This approach is justified because the denominator in the fraction already incorporates the nonlinear parameters into the expression, as discussed in the works of [21,36,40]. Therefore, in Equation (4), our analysis is limited to the classical dipole magnetic field, which can be expressed using the magnetic induction  $\mathbf{m}$ , located at the coordinate origin, as follows:

$$\vec{B} = \frac{3(\mathbf{m} \cdot \mathbf{r})\mathbf{r}}{r^5} - \frac{\mathbf{m}}{r^3}, \quad (5)$$

We will consider a simplified scenario in which the light ray passes through the equatorial plane of the magnetic dipole, as depicted in Figure 1.

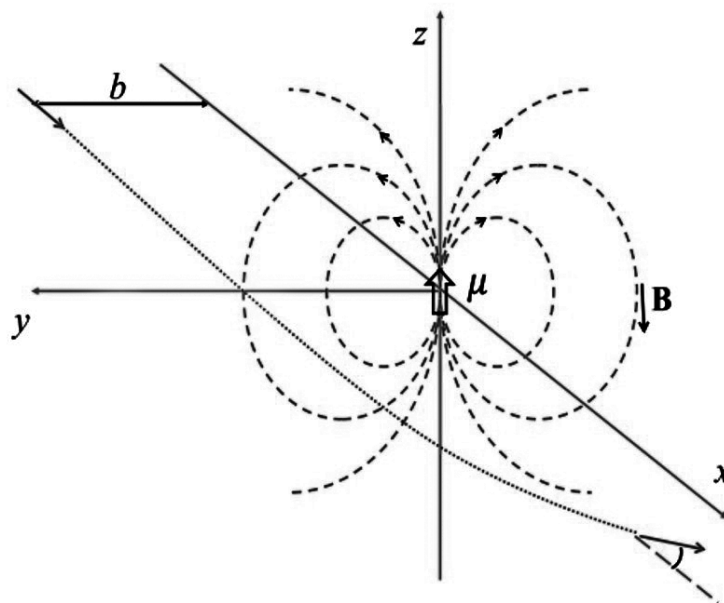


**Figure 1.** A diagram illustrating the bending of light when a ray of light passes through the equatorial plane of a magnetic dipole is shown [21].

### 3. The Bending Angle via the Gauss–Bonnet Theorem

Assuming that the magnetic dipole direction serves as the  $z$ -axis, denoted by  $\mathbf{m} = \mu\hat{z}$ , the magnetic field at the equator can be expressed as follows:

$$\bar{\mathbf{B}} = -\frac{\mu\hat{z}}{r^3}, \quad (6)$$

where  $r = \sqrt{x^2 + y^2}$ , and  $\hat{z}$  is a unit vector along the  $z$ -axis. The indices of refraction (4) can be rewritten as

$$n_{\perp} \approx 1 + \frac{\mu^2}{2\beta^2 r^6}, \quad n_{\parallel} \approx 1 + \frac{\mu^2}{2\gamma^2 r^6}. \quad (7)$$

Several methods exist for both the approximate and exact determination of the light deflection angle, such as the null geodesics approach, which applies either perturbation procedures [41,42] or the direct integration of the null geodesic equations [43–45]. In particular, the motion of light in a non-uniform medium closely resembles how a physical object moves in a potential field. This approach allows for highly accurate descriptions of how the light's direction changes in various spacetimes [14–17]. As a result, we can effectively assign a refractive index to the surrounding field. In [46], the authors introduced an alternative calculation method that utilises the concept of the refractive index of optical media in combination with the Gauss–Bonnet theorem applied to isotropic optical metrics, leading to an exact result for the deflection angle in both Kerr and Teo wormhole geometries.

On the equatorial plane, the refractive index does not rely on the  $z$ -coordinate, implying that, at the equator,  $\bar{\mathbf{B}} = \bar{\mathbf{B}}(x, y)$ . We then calculate the angle of bending in the  $y$ -direction for the perpendicular mode, applying the weak bending approximation, as referenced in [21], using optical geometries. However, to calculate the bending angle, we will use the Gauss–Bonnet Theorem (GBT), originally stated in [46–48].

$$\iint_D \mathcal{K} dS + \sum_{a=1}^N \int_{\partial D_a} k_g dl + \sum_{a=1}^N \theta_a = 2\pi\chi(D). \quad (8)$$

In this context, the domain  $D$  is characterised by a Gaussian curvature  $\mathcal{K}$ , represented by a freely orientable curved surface  $S$  with an infinitesimal area element  $dS$ . The boundaries of  $D$  are indicated by  $\partial D_a$ , with a range from 1 to  $N$ . The geodesic curvature  $k_g$  is taken into account along the path  $dl$ , adhering to a positive convention. Furthermore,  $\theta_a$  signifies the jump angle, and  $\chi(D)$  represents the Euler characteristic. In this instance, it equals 1, indicating that  $D$  is located in a nonsingular region. It was shown by [49] that, in a static spherically symmetric spacetime exhibiting asymptotic flatness, Equation (8) can be written as

$$\Delta\theta_{\perp} = -\iint_D^m \mathcal{K} dS. \quad (9)$$

Following [46], the expression for the Gaussian optical curvature  $\mathcal{K}$  is represented in terms of the coordinates and the refraction index as follows:

$$\mathcal{K} = -\frac{n(r)n''(r)r - (n'(r))^2 r + n(r)n'(r)}{n^4(r)r}. \quad (10)$$

Substituting the expression for the effective refractive index for the perpendicular mode in Equation (7), we obtain the result

$$\mathcal{K} = \frac{18\mu^2}{\beta^2 r^8}. \quad (11)$$

By utilising the light-ray equation  $r = b/\sin \varphi$ , also using (11) and  $dS = n^2(r)rdrd\varphi$ , (9) becomes

$$\begin{aligned}\Delta\theta_{\perp} &= -\int_0^{\pi} \int_{\frac{b}{\sin\varphi}}^{\infty} \frac{18\mu^2}{\beta^2 r^8} \left(1 + \frac{\mu^2}{2\beta^2 r^6}\right)^2 r dr d\varphi \\ &\approx -\int_0^{\pi} \int_{\frac{b}{\sin\varphi}}^{\infty} \frac{18\mu^2}{\beta^2 r^7} dr d\varphi.\end{aligned}\quad (12)$$

Thus, the bending-angle expression of the generalised Born–Infeld electrodynamics is

$$\Delta\theta_{\perp} = -\frac{15\pi}{16} \frac{\mu^2}{\beta^2 b^6}, \quad (13)$$

where  $b$  is the impact parameter, and the negative sign indicates that bending occurs toward the magnetic dipole. The above equation represents the bending angle of light in the GBI NED on the order of the parameter  $\beta^{-2}$ . This parameter incorporates two additional parameters, as given in Equation (2). Specifically, when  $\beta_0 \rightarrow \infty$ , Equation (13) simplifies to the bending angle of EH NED, as follows:

$$\Delta\theta_{\perp} = \frac{\pi}{3} \frac{\alpha^2}{m_e^4} \frac{\mu^2}{b^6}, \quad (14)$$

and the parallel mode becomes  $\Delta\theta_{\parallel} = (7/4)\Delta\theta_{\perp}$ . This results precisely aligns with the bending angle derived from the Euler–Heisenberg Lagrangian [18,50].

#### 4. Estimating the Deflection Angle of Magnetars from the McGill Catalog

As previously mentioned in the introduction, despite the challenges associated with conducting laboratory experiments to test the effects of nonlinear vacuum electrodynamics, which requires the generation of extremely high critical fields, there exists a distinctive opportunity to study these phenomena. This opportunity is presented by observational astrophysics. The most remarkable magnetic fields known in the observable universe are located in neutron stars known as magnetars. In the modern era, 29 magnetars have been discovered within our galaxy, and 2 have been found outside of it [51]. Among these, 26 have been officially classified as magnetars, while 5 are considered potential candidates [51,52]. The McGill Online Magnetar Catalog [53,54] has greatly facilitated the creation of a distribution map using the Aitoff–Hammer projection, and it is clear that magnetars align along the galactic plane, with their positions represented by black crosses in Figure 2.

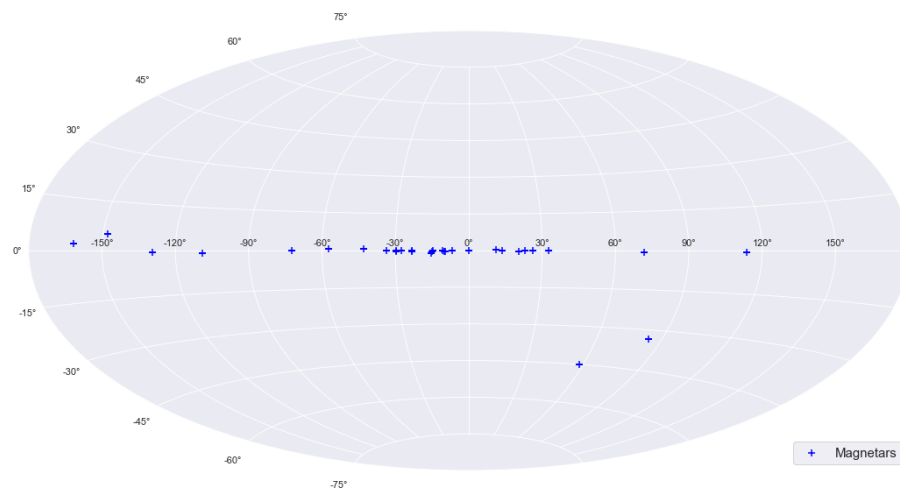


Figure 2. Distribution map of the magnetars in Aitoff projection [55].

Table 1 shows the numerical estimate of each bending angle  $\Delta\theta_{\perp}$  in Equation (17) for the arbitrary values  $r_s$  and the magnetic fields corresponding to 24 galactic magnetars [55].

**Table 1.** Numerical estimation of each bending angle in Equation (17) for the arbitrary values  $r_s$  and the magnetic fields corresponding to 24 galactic magnetars [52,55].

Magnetar Name	$B_s$	$b = r_s$ $\Delta\theta_{\perp}$	$b = 3r_s$ $\Delta\theta_{\perp}$	$b = 6r_s$ $\Delta\theta_{\perp}$	$b = 10r_s$ $\Delta\theta_{\perp}$
CXOU J010043.1-721134	$3.93 \times 10^{10}$	—	$6.65 \times 10^{-5}$	$1.04 \times 10^{-6}$	$4.85 \times 10^{-8}$
4U 0142+61	$1.34 \times 10^{10}$	—	$7.74 \times 10^{-6}$	$1.21 \times 10^{-7}$	$5.64 \times 10^{-9}$
SGR 0418+5729	$6.10 \times 10^8$	$1.17 \times 10^{-5}$	$1.60 \times 10^{-8}$	$2.51 \times 10^{-10}$	$1.17 \times 10^{-11}$
SGR 0501+4516	$1.87 \times 10^{10}$	—	$1.51 \times 10^{-5}$	$2.35 \times 10^{-7}$	$1.10 \times 10^{-8}$
SGR 0526-66	$5.60 \times 10^{10}$	—	$1.35 \times 10^{-4}$	$2.11 \times 10^{-6}$	$9.85 \times 10^{-8}$
1E 1048.1-5937	$3.86 \times 10^{10}$	—	$6.42 \times 10^{-5}$	$1.00 \times 10^{-6}$	$4.68 \times 10^{-8}$
1E 1547.0-5408	$3.18 \times 10^{10}$	—	$4.36 \times 10^{-5}$	$6.81 \times 10^{-7}$	$3.18 \times 10^{-8}$
PSR J1622-4950	$2.74 \times 10^{10}$	—	$3.23 \times 10^{-5}$	$5.05 \times 10^{-7}$	$2.36 \times 10^{-8}$
SGR 1627-41	$2.25 \times 10^{10}$	—	$2.18 \times 10^{-5}$	$3.41 \times 10^{-7}$	$1.59 \times 10^{-8}$
CXOU J164710.2-455216	$6.59 \times 10^9$	—	$1.87 \times 10^{-6}$	$2.92 \times 10^{-8}$	$1.36 \times 10^{-9}$
1RXS J170849.0-400910	$4.68 \times 10^{10}$	—	$9.44 \times 10^{-5}$	$1.47 \times 10^{-6}$	$6.88 \times 10^{-8}$
CXOU J171405.7-381031	$5.01 \times 10^{10}$	—	$1.08 \times 10^{-4}$	$1.69 \times 10^{-6}$	$7.88 \times 10^{-8}$
SGR J1745-2900	$2.31 \times 10^{10}$	—	$2.30 \times 10^{-5}$	$3.59 \times 10^{-7}$	$1.68 \times 10^{-8}$
SGR 1806-20	$1.96 \times 10^{11}$	—	—	$2.59 \times 10^{-5}$	$1.21 \times 10^{-6}$
XTE J1810-197	$2.10 \times 10^{10}$	—	$1.90 \times 10^{-5}$	$2.97 \times 10^{-7}$	$1.39 \times 10^{-8}$
Swift J1818.0-1607	$3.54 \times 10^{10}$	—	$5.40 \times 10^{-5}$	$8.44 \times 10^{-7}$	$3.94 \times 10^{-8}$
Swift J1822.3-1606	$1.36 \times 10^9$	$5.81 \times 10^{-5}$	$7.97 \times 10^{-8}$	$1.25 \times 10^{-9}$	$5.81 \times 10^{-11}$
SGR 1833-0832	$1.65 \times 10^{10}$	—	$1.17 \times 10^{-5}$	$1.83 \times 10^{-7}$	$8.55 \times 10^{-9}$
Swift J1834.9-0846	$1.42 \times 10^{10}$	—	$8.69 \times 10^{-6}$	$1.36 \times 10^{-7}$	$6.33 \times 10^{-9}$
1E 1841-045	$7.03 \times 10^{10}$	—	$2.13 \times 10^{-4}$	$3.33 \times 10^{-6}$	$1.55 \times 10^{-7}$
3XMM J185246.6+003317	$4.07 \times 10^9$	$5.20 \times 10^{-4}$	$7.14 \times 10^{-7}$	$1.12 \times 10^{-8}$	$5.20 \times 10^{-10}$
SGR 1900+14	$7.00 \times 10^{10}$	—	$2.11 \times 10^{-4}$	$3.30 \times 10^{-6}$	$1.54 \times 10^{-7}$
SGR 1935+2154	$2.18 \times 10^{10}$	—	$2.05 \times 10^{-5}$	$3.20 \times 10^{-7}$	$1.49 \times 10^{-8}$
1E 2259+586	$5.88 \times 10^9$	—	$1.49 \times 10^{-6}$	$2.33 \times 10^{-8}$	$1.09 \times 10^{-9}$

Following the notation in [21], the total bending angle caused by magnetars can be expressed in the order of the impact parameter:

$$\Delta\theta = \Delta\theta_1 - \Delta\theta_2 + \Delta\theta_3, \quad (15)$$

where  $\Delta\theta_1$  represents the bending angle caused by gravitational mass, and  $\Delta\theta_2$  and  $\Delta\theta_3$  are the bending angles including the NED effect.

Now, let us provide an estimate of the bending angle for the magnetars listed in Table 1. We will consider the deflection of light by a typical neutron star with a mass of  $M = 1.4M_{\odot}$ . To this end, we first restore all normalised units and rewrite the expressions for the angle of deviation from Equation (14):

$$\Delta\theta_{\perp} = \frac{\alpha^2 \pi}{3m_e^4} \left( \frac{\hbar^3 \epsilon_0}{c^3} \right) \left( \frac{\mu_0}{4\pi} \right)^2 \left( \frac{\mu^2}{b^6} \right). \quad (16)$$

It is more useful to express  $\Delta\theta_{\perp}$  in terms of the magnetic induction on the magnetar surface and the critical QED field strength as

$$\Delta\theta_{\perp} = \frac{\alpha B_s^2 r_s^6}{12 B_c^2 b^6}, \quad (17)$$

where  $r_s$  is the radius of the magnetar,  $B_s = \left( \frac{\mu_0}{4\pi} \right) \left( \frac{\mu}{r_s^3} \right)$ ,  $B_c = m_e^2 c^2 / e \hbar = 4.4 \times 10^9$  T, and  $\alpha = e^2 / 4\pi \epsilon_0 \hbar c$ .

In [21], it was demonstrated that near the equator of the magnetar, the bending caused by the NED effect, as represented by  $\Delta\theta_3$ , is comparable to gravitational lensing by mass  $\Delta\theta_1$ . Meanwhile, the  $\Delta\theta_2$  term is negligible in conditions where the maximum surface

magnetic field  $B_s = 10^{11}$  T and  $b \simeq r_s$ . In our case, we calculated the bending angle of the NED term under the condition  $B < B_c$  (which is the equivalent condition for the GBI parameter  $\bar{B}^2/\beta^2 < 1$ ); therefore, Equation (17) is not applicable to most of the magnetars in the list of the McGill catalogue at the magnetar surface  $b \simeq r_s$ .

To observe the NED effect on the bending angle  $\Delta\theta_3$ , it is reasonable to compare it with the bending angle caused by the gravitational term for the same object in the same context. We limit our discussion to the weak bending angle of light, i.e., to cases of weak gravitational bending where the impact parameter is large in comparison to the Schwarzschild radius, denoted by  $b = r_s \gg r_g$ . Then, in Equation (15), the main term for the bending angle due to gravitational mass can be expressed as follows:

$$\Delta\theta_1 = \frac{4GM}{c^2 b}. \quad (18)$$

Table 2 shows the gravitational term of the deflection angle, which is calculated by  $\Delta\theta_1$  in Equation (15), in the regime of a weak gravitational field corresponding to the impact parameters.

**Table 2.** The gravitational term of deflection angle, which is calculated by  $\Delta\theta_1$  in Equation (18).

$b$	$b = r_s$	$b = 3r_s$	$b = 6r_s$	$b = 10r_s$
$\Delta\theta_s$	$8.28 \times 10^{-1}$	$2.76 \times 10^{-1}$	$1.38 \times 10^{-1}$	$8.28 \times 10^{-2}$

## 5. Conclusions

In this work, we studied the effect of a weak bending angle in the context of NED. By using the refractive index corresponding to the dipole in the framework of GBI, we calculated the Gaussian optical curvature based on the refractive indices. Using the obtained Gaussian optical curvature and the principles of the Gauss–Bonnet theorem, we derived a formula for the deflection angle in a magnetic field of a dipole. Despite the fact that the same results can be obtained using the trajectory equation based on geometric optics principles, the Gauss–Bonnet theorem demonstrates itself to be a robust mathematical tool in modern theoretical research, which can be applied to consider more complex cases when standard methods for obtaining solutions collide with significant difficulties.

The expression for the deflection angle obtained theoretically was applied to magnetars from the McGill catalogue to estimate the order of magnitude of the light deflection angle of the NED term. As a result, at the surface of the star ( $b = r_s$ ), because the magnitude of the magnetic field is greater than that of the characteristic magnetic field  $B_s > B_c$  (or does not satisfy the condition for the NED parameter  $\bar{B}^2/\beta^2 < 1$  in Equation (4)), the above expression Equation (17) is applicable only to a few magnetars, i.e., SGR 0418+5729, Swift J1822.3-1606, and 3XMM J185246.6+003317. At long distances, this calculation is suitable for determining the bending angle's NED term for all magnetars listed in the McGill catalogue. The results obtained are significantly smaller than the gravitational component of the bending angle, even for a weak gravitational field, when considering the same distance.

However, for a complete and correct comparison of the astrophysical effects of NED, it is necessary to calculate an exact combined metric. For this reason, in future works, we will consider the deflection of a light beam by modified Lagrangians [56–58].

**Author Contributions:** Conceptualisation, M.K. and S.T.; methodology, T.Y., A.T. (Aliya Taukenova) and A.T. (Amankhan Talkhat); validation, N.B., A.T. (Aliya Taukenova) and A.T. (Amankhan Talkhat); formal analysis, M.K., T.Y., S.T. and N.B.; investigation, T.Y., M.K. and S.T.; writing—original draft preparation, T.Y., M.K. and S.T.; writing—review and editing, M.K. and S.T.; resources: T.Y., A.T. (Aliya Taukenova) and N.B.; funding acquisition, M.K. and N.B. All authors have read and agreed to the published version of the manuscript.

**Funding:** This research was funded by the Ministry of Science and Higher Education of the Republic of Kazakhstan (Grant No. AP14972943).

**Institutional Review Board Statement:** Not applicable.

**Informed Consent Statement:** Not applicable.

**Data Availability Statement:** Data are contained within the article.

**Acknowledgments:** This research was funded by the Ministry of Science and Higher Education of the Republic of Kazakhstan (Grant No. AP14972943). We would like to extend our sincere appreciation to J.Y. Kim and M.E. Abishev for their valuable discussions.

**Conflicts of Interest:** The authors declare no conflicts of interest.

## References

1. Born, M.; Infeld, L. Foundations of the New Field Theory. *Proc. R. Soc. Lond. Ser. A* **1934**, *144*, 425–451. [[CrossRef](#)]
2. Born, M. On the Quantum Theory of the Electromagnetic Field. *Proc. R. Soc. Lond. Ser. A* **1934**, *143*, 410–437. [[CrossRef](#)]
3. Beissen, N.; Abishev, M.; Toktarbay, S.; Yernazarov, T.; Utepova, D.; Zhakipova, M. The Exploring nonlinear vacuum electro-dynamics beyond Maxwell's Equations. *Int. J. Math. Phys.* **2023**, *14*, 61–70. [[CrossRef](#)]
4. Heisenberg, W.; Euler, H. Folgerungen aus der Diracschen Theorie des Positrons. *Z. Phys.* **1936**, *98*, 714–732. [[CrossRef](#)]
5. Schwinger, J. On Gauge Invariance and Vacuum Polarization. *Phys. Rev.* **1951**, *82*, 664–679. [[CrossRef](#)]
6. Jackson, J.D.; Fox, R.F. Classical Electrodynamics, 3rd ed. *Am. J. Phys.* **1999**, *67*, 841–842. [[CrossRef](#)]
7. Cameron, R.; Cantatore, G.; Melissinos, A.; Ruoso, G.; Semertzidis, Y.; Halama, H.; Lazarus, D.; Prodell, A.; Nezrick, F.; Rizzo, C.; et al. Search for nearly massless, weakly coupled particles by optical techniques. *Phys. Rev. D* **1993**, *47*, 3707. [[CrossRef](#)]
8. Della Valle, F.; Milotti, E.; Ejlli, A.; Messineo, G.; Piemontese, L.; Zavattini, G.; Gastaldi, U.; Pengo, R.; Ruoso, G. First results from the new PVLAS apparatus: A new limit on vacuum magnetic birefringence. *Phys. Rev. D* **2014**, *90*, 092003. [[CrossRef](#)]
9. Cadène, A.; Berceau, P.; Fouché, M.; Battesti, R.; Rizzo, C. Vacuum magnetic linear birefringence using pulsed fields: Status of the BMV experiment. *Eur. Phys. J. D* **2014**, *68*, 16. [[CrossRef](#)]
10. Rasheed, D. Non-linear electrodynamics: Zeroth and first laws of black hole mechanics. *arXiv* **1997**, arXiv:hep-th/9702087.
11. Garcia-Salcedo, R.; Breton, N. Born–Infeld cosmologies. *Int. J. Mod. Phys. A* **2000**, *15*, 4341–4353. [[CrossRef](#)]
12. Bretón, N. Born-Infeld black hole in the isolated horizon framework. *Phys. Rev. D* **2003**, *67*, 124004. [[CrossRef](#)]
13. Camara, C.; de Garcia Maia, M.; Carvalho, J.; Lima, J.A.S. Nonsingular FRW cosmology and nonlinear electrodynamics. *Phys. Rev. D* **2004**, *69*, 123504. [[CrossRef](#)]
14. Alsing, P. The optical-mechanical analogy for stationary metrics in general relativity. *Am. J. Phys.* **1998**, *66*, 779–790. [[CrossRef](#)]
15. Roy, S.; Sen, A. Trajectory of a light ray in Kerr field: A material medium approach. *Astrophys. Space Sci.* **2015**, *360*, 23. [[CrossRef](#)]
16. Toktarbay, S.; Quevedo, H.; Abishev, M.; Muratkhon, A. Gravitational field of slightly deformed naked singularities. *Eur. Phys. J. C* **2022**, *82*, 382. [[CrossRef](#)]
17. Beissen, N.; Utepova, D.; Abishev, M.; Quevedo, H.; Khassanov, M.; Toktarbay, S. Gravitational Refraction of Compact Objects with Quadrupoles. *Symmetry* **2023**, *15*, 614. [[CrossRef](#)]
18. Denisov, V.I.; Denisova, I.P.; Svertilov, S.I. Nonlinear Electrodynamical Effect of Ray Bending in the Magnetic-Dipole Field. *Dokl. Phys.* **2001**, *46*, 705–707. [[CrossRef](#)]
19. Denisov, V.I.; Denisova, I.P.; Svertilov, S.I. The nonlinear-electrodynamical bending of the x-ray and gamma-ray in the magnetic field of pulsars and magnetars. *arXiv* **2001**, arXiv:astro-ph/0110705.
20. Abishev, M.E.; Toktarbay, S.; Beissen, N.A.; Belissarova, F.B.; Khassanov, M.; Kodussov, A.S.; Abylayeva, A.Z. Effects of non-linear electrodynamics of vacuum in the magnetic quadrupole field of a pulsar. *Mon. Not. R. Astron. Soc.* **2018**, *481*, 36–43. [[CrossRef](#)]
21. Kim, J.Y. Deflection of light by magnetars in the generalized Born–Infeld electrodynamics. *Eur. Phys. J. C* **2022**, *82*, 485. [[CrossRef](#)]
22. Gibbons, G.; Werner, M. Applications of the Gauss–Bonnet theorem to gravitational lensing. *Class. Quantum Gravity* **2008**, *25*, 235009. [[CrossRef](#)]
23. Werner, M. Gravitational lensing in the Kerr–Randers optical geometry. *Gen. Relativ. Gravit.* **2012**, *44*, 3047–3057. [[CrossRef](#)]
24. Jusufi, K.; Werner, M.C.; Banerjee, A.; Övgün, A. Light deflection by a rotating global monopole spacetime. *Phys. Rev. D* **2017**, *95*, 104012. [[CrossRef](#)]
25. Jusufi, K.; Övgün, A. Gravitational lensing by rotating wormholes. *Phys. Rev. D* **2018**, *97*, 024042. [[CrossRef](#)]
26. Jusufi, K.; Sakalli, İ.; Övgün, A. Effect of Lorentz symmetry breaking on the deflection of light in a cosmic string spacetime. *Phys. Rev. D* **2017**, *96*, 024040.
27. Jusufi, K.; Övgün, A.; Saavedra, J.; Vásquez, Y.; Gonzalez, P. Deflection of light by rotating regular black holes using the Gauss–Bonnet theorem. *Phys. Rev. D* **2018**, *97*, 124024. [[CrossRef](#)]
28. Jusufi, K.; Övgün, A. Effect of the cosmological constant on the deflection angle by a rotating cosmic string. *Phys. Rev. D* **2018**, *97*, 064030. [[CrossRef](#)]
29. Javed, W.; Hamza, A.; Övgün, A. Effect of nonlinear electrodynamics on the weak field deflection angle by a black hole. *Phys. Rev. D* **2020**, *101*, 103521. [[CrossRef](#)]
30. Moumni, H.E.; Masmari, K.; Övgün, A. Weak Deflection angle of some classes of non-linear electrodynamics black holes via Gauss–Bonnet Theorem. *arXiv* **2020**, arXiv:2008.06711.
31. Gaete, P.; Helayël-Neto, J. Remarks on nonlinear electrodynamics. *Eur. Phys. J. C* **2014**, *74*, 3182. [[CrossRef](#)]



32. Kruglov, S.I. Notes on Born-Infeld-type electrodynamics. *Mod. Phys. Lett. A* **2017**, *32*, 1750201. [[CrossRef](#)]
33. Bandos, I.; Lechner, K.; Sorokin, D.; Townsend, P.K. Nonlinear duality-invariant conformal extension of Maxwell's equations. *Phys. Rev. D* **2020**, *102*, 121703. [[CrossRef](#)]
34. Kruglov, S.I. On generalized ModMax model of nonlinear electrodynamics. *Phys. Lett. B* **2021**, *822*, 136633. [[CrossRef](#)]
35. Belmar-Herrera, S.; Balart, L. Charged black holes from a family of Born-Infeld-type electrodynamics models. *Mod. Phys. Lett. A* **2022**, *37*, 2250194. [[CrossRef](#)]
36. Kruglov, S.I. On generalized Born-Infeld electrodynamics. *J. Phys. A Math. Gen.* **2010**, *43*, 375402. [[CrossRef](#)]
37. Ahlers, M.; Gies, H.; Jaeckel, J.; Redondo, J.; Ringwald, A. Laser experiments explore the hidden sector. *Phys. Rev. D* **2008**, *77*, 095001. [[CrossRef](#)]
38. Zavattini, E.; Zavattini, G.; Ruoso, G.; Polacco, E.; Milotti, E.; Karuza, M.; Gastaldi, U.; Di Domenico, G.; Della Valle, F.; Cimino, R.; et al. Experimental Observation of Optical Rotation Generated in Vacuum by a Magnetic Field. *Phys. Rev. Lett.* **2006**, *96*, 110406. [[CrossRef](#)]
39. Born, M.; Infeld, L. Foundations of the New Field Theory. *Nature* **1933**, *132*, 1004. [[CrossRef](#)]
40. Denisov, D.M. Effects of nonlinear electrodynamics in the magnetic field of a pulsar. *Can. J. Phys.* **2014**, *92*, 1453–1459. [[CrossRef](#)]
41. Misner, C.W.; Thorne, K.S.; Wheeler, J. *Gravitation*; W. H. Freeman and Company: New York, NY, USA, 1971.
42. Ray, D. *Introducing Einsteins Relativity*; Oxford University Press: Oxford, UK, 1998.
43. Chandrasekhar, S. *The Mathematical Theory of Black Holes*; Oxford University Press: Oxford, UK, 1983.
44. Weinberg, S. *Gravitation and Cosmology*; John Wiley and Sons Inc.: Hoboken, NJ, USA, 1972.
45. Wald, R. *General Relativity*; University of Chicago Press: Chicago, IL, USA, 1984.
46. Jusufi, K. Gravitational deflection of relativistic massive particles by Kerr black holes and Teo wormholes viewed as a topological effect. *Phys. Rev. D* **2018**, *98*, 064017. [[CrossRef](#)]
47. Do Carmo, M.P. *Differential Geometry of Curves and Surfaces: Revised and Updated*, 2nd ed.; Courier Dover Publications: Mineola, NY, USA, 2016.
48. Klingenberg, W. *A Course in Differential Geometry*; Springer Science & Business Media: Berlin/Heidelberg, Germany, 2013; Volume 51.
49. Ishihara, A.; Suzuki, Y.; Ono, T.; Kitamura, T.; Asada, H. Gravitational bending angle of light for finite distance and the Gauss-Bonnet theorem. *Phys. Rev. D* **2016**, *94*, 084015. [[CrossRef](#)]
50. Kim, J.Y.; Lee, T. Light bending by nonlinear electrodynamics under strong electric and magnetic field. *J. Cosmol. Astropart. Phys.* **2011**, *2011*, 017. [[CrossRef](#)]
51. Kaspi, V.M.; Beloborodov, A.M. Magnetars. *Annu. Rev. Astron. Astrophys.* **2017**, *55*, 261–301. [[CrossRef](#)]
52. Yernazarov, T.; Abishev, M.; Aimuratov, Y. Correspondence of gamma radiation coming from GRBs and magnetars based on the effects of nonlinear vacuum electrodynamics. In Proceedings of the Sixteenth Marcel Grossmann Meeting on Recent Developments in Theoretical and Experimental General Relativity, Astrophysics and Relativistic Field Theories: Proceedings of the MG16 Meeting on General Relativity, Online, 5–10 July 2021; World Scientific: Singapore, 2023; pp. 4401–4409.
53. Pereira, J.P.; Coelho, J.G.; de Lima, R.C. Born-Infeld magnetars: Larger than classical toroidal magnetic fields and implications for gravitational-wave astronomy. *Eur. Phys. J. C* **2018**, *78*, 361. [[CrossRef](#)]
54. Group, M.P. McGill Online Magnetar Catalog. Available online: <http://www.physics.mcgill.ca/~pulsar/magnetar/main.html> (accessed on 17 November 2020).
55. Olausen, S.A.; Kaspi, V.M. The McGill Magnetar Catalog. *APJS* **2014**, *212*, 6. [[CrossRef](#)]
56. Shabad, A.E.; Usov, V.V. Effective Lagrangian in nonlinear electrodynamics and its properties of causality and unitarity. *Phys. Rev. D* **2011**, *83*, 105006. [[CrossRef](#)]
57. Avetisyan, Z.; Evnin, O.; Mkrtchyan, K. Democratic Lagrangians for Nonlinear Electrodynamics. *Phys. Rev. Lett.* **2021**, *127*, 271601. [[CrossRef](#)] [[PubMed](#)]
58. Kruglov, S.I. Nonlinear arcsin-electrodynamics. *Ann. Der Phys.* **2015**, *527*, 397–401. [[CrossRef](#)]

**Disclaimer/Publisher's Note:** The statements, opinions and data contained in all publications are solely those of the individual author(s) and contributor(s) and not of MDPI and/or the editor(s). MDPI and/or the editor(s) disclaim responsibility for any injury to people or property resulting from any ideas, methods, instructions or products referred to in the content.